

DIFFERENCES IN THE FREQUENCY AND DISTRIBUTION OF INTENSE EXTRATROPICAL CYCLONE EVENTS IN A MODEL- SIMULATED DOUBLED CO₂ ENVIRONMENT

Kristopher L. Wile*

University of Wisconsin-Madison, Madison, Wisconsin

1. INTRODUCTION AND BACKGROUND

It has been well documented (Chang & Fu, 2002, Lim & Simmonds, 2002, Lim & Simmonds, 2003, 2004, Carnell, 1998) that within the last one hundred fifty years the Earth has been experiencing a prolonged period of increasing mean global surface temperature (~2°C). This observed “global warming” can be attributed to a combination of many factors both naturally and anthropogenically induced. The breakdown of the causes of this warming is beyond the scope of this presentation, despite being a very relevant and controversial topic. Instead, the purpose of this talk is to further investigations, such as those of Lambert, 1995, 1996, Lim & Simmonds, 2002, 2004, and Schubert, 1998 regarding how the frequency and distribution of extreme Northern Hemisphere (NH) extratropical storms might be affected given a greenhouse warming scenario.

Midlatitude cyclones are among the most important circulation systems involved in the transport of heat and moisture polewards away from the tropical regions. Thus changes in the frequency, intensity, and distribution of NH extratropical cyclones under a global warming scenario will likely impact the manner in which heat and moisture are dispersed throughout the hemisphere. Such changes in future weather patterns could potentially have a large global socioeconomic impact. This study will particularly focus upon changes to the most intense of these NH extratropical cyclones that we shall term “intense cyclone events” (ICEs) - which are cyclones with a central sea-level pressure of 970 hPa or less for a significant portion of their life cycle.

A global warming scenario does not imply an even distribution of the warming across all latitudes and longitudes on the Earth. In fact, the observations strongly suggest that the warming is

actually greatly amplified at high latitudes compared to the low latitudes (IPCC, 2001). This polar amplification effect, created as a consequence of a non-uniform albedo feedback, will result in a reduced pole to equator temperature gradient, thus greatly reducing the mean baroclinicity of the NH. Given that mid-latitude cyclones derive their energy from the background baroclinicity it is quite likely that a reduction in the intensity of that baroclinicity will result in some notable alteration in the frequency, intensity, and distribution of extratropical cyclones in such a warming scenario. There have been several different experiments with various numerical models (Lambert, 1995, 1996, Sinclair, 1999, Zhang & Wang, 1997, Geng & Sugi, 2001, 2003, Knipperitz et al., 2000, Carnell, 1996, 1998) whose results support the claim that there will be a reduced number of storms in the NH. The more complicated and less obvious conclusion is that there may actually be an increase in the number of intense cyclones (Knipperitz et al., 2000, Lim & Simmonds, 2002, 2004, Lambert, 1995, 1996, Geng & Sugi, 2001, 2003, Carnell, 1996, 1998, Zhang & Walsh 2004). Though such a conclusion is potentially connected to the operational definition of “intense cyclones” (defined in Section 2) there may truly be a significant increase in ICEs in a global warming scenario. It is not at all clear why this might be the case. Additionally, if there is a significant increase in ICEs in a warmer climate, it is not currently known how the structure of these cyclones might differ from such events found in the present climate.

Northern Hemisphere baroclinicity can be defined in various ways. One way is lower tropospheric horizontal baroclinicity, which is used by surface cyclones as an energy source for intensification. Differences in atmospheric lapse rates throughout the depth of the troposphere are an indicator of the static stability of any given layer within the atmosphere. A greenhouse warming scenario will not only raise the mean horizontal temperature across the globe, but also dramatically alter the vertical temperature profiles and thus, in turn, the stability of the atmosphere. With warmer temperatures a likely possibility is

* Corresponding author address: Kristopher L. Wile, Univ. of Wisconsin-Madison, Dept. of Atmos. & Ocn. Sciences, Madison, WI 53706, e-mail: kristopher_wile@yahoo.com

weaker static stability especially in the low levels of the troposphere, which allows for more vertical mixing. The strength of the vertical mixing is a gauge of atmospheric overturning and instability. Enhanced vertical mixing allows extratropical cyclones to strengthen throughout the depth of the troposphere, which allows vertical coupling to occur. Vertical coupling is an important mechanism that allows extratropical cyclones to more efficiently strengthen. Finally another aspect of NH baroclinicity that will be greatly affected in the global warming scenario is the large-scale hemispheric meridional baroclinicity. This is exemplified by the pole-to-equator temperature gradient, which will be greatly reduced thus dramatically decreasing the main energy source for NH extratropical cyclones. The effect of all these changes to the temperature gradients both in the horizontal, vertical, and throughout the hemisphere on the structure of extratropical storms is currently an open question.

The method that will be invoked in exploring changes in NH extratropical cyclones will be an examination of GCM model output. GCMs come in many varieties with complex physics regimes, various parameterizations and resolutions. The differences between GCMs allow certain GCMs to simulate certain climate regime changes better than others. However, there is no specific rule of thumb; just because a model has a higher spatial or temporal resolution, it does not necessarily mean it is a "better" model. Each model has to be evaluated on an individual basis for a specific experiment and then determine what model is best representative of the induced changes. That is why model intercomparisons and model ensembles have great value. They allow the user to realize if a GCM is biased in any way or if it is representative of a majority of the GCMs (Schubert, 1998). Obviously there are advantages and disadvantages to using only one GCM or many GCMs. Understanding how a particular model behaves given various experiments can be very insightful in determining how physical processes can change within that model but the model might be biased in some way. Using an ensemble of models usually alleviates the model bias, but makes it much more difficult to understand changes in the individual model physics. The Intergovernmental Panel of Climate Change (IPCC) has chosen some of the most comprehensive, physically reasonable, and best representative of the real world GCMs to better understand the past, present, and future climate scenarios including the GFDL_CM2.0 (Delworth,

2004, GFDL, 2004) which is the GCM used for the analysis in this presentation.

One of the key differences between models is horizontal, vertical, and temporal resolution. One might expect that the finer the resolution, the more accurate depiction of the climate can be made (Schubert, 1998), though this rule does not always apply. However, at the expense of finer resolution, the model run becomes orders of magnitude more computationally expensive. That is why a balance between resolution and computational power needs to be struck based upon the phenomenon that is at the core of the study. In this case, extratropical cyclones which have a time scale of a couple of days to a couple of weeks would be best represented by 12-hourly or 24-hourly data and obviously not monthly mean data. Also looking at a long time series of how these cyclones adjust to a warmer climate is important, thus a single year of data will not nearly give as accurate a representation as a ten or twenty year model run. The spatial scale also is best represented by a higher horizontal and vertical resolution model. All of these synoptic/climatic characteristics were accounted for and seem to be best incorporated by the GFDL_CM2.0. Its specifications will be addressed in the next section.

NH extratropical cyclones have preferred geographical regions for formation and occurrence. This is what is classically called the Northern Hemisphere Storm Track (NHST). The NHST also has a more specific definition but it depends upon which study and diagnostic was chosen. Carnell et al. (1996) defines high frequency variability (HFV) as 2-6 day frequency. Regions with maximum HFV that stretch zonally across the North Atlantic and the North Pacific are defined as the Storm Tracks (STs). Schubert, et al. (1998) defines the storm track as the area of enhanced variance of band-pass filtered (2.5-6 day) 500hPa geopotential height. Sinclair et al. (1999) uses a looser definition of the area directly south of the climatological polar jet axis over the North Pacific from Japan to the Gulf of Alaska and North Atlantic from North America into the Arctic Ocean. All of these definitions have merit and are useful for their particular studies. In reality, using any one, or a combination of these definitions, places the ST over the same location with little difference. For the rest of this presentation, the Sinclair definition will be used for clarity and geographical distinction.

The climatological ST is where the lion's share of the NH extratropical cyclones are located. This occurs as a result of the large baroclinic zone

located on the western edge of the ocean basins where continental airmasses are forced out over open ocean and create or more fully develop cyclones. The NHST can be broken down into two sub regions of focus, the North Atlantic Storm Track (NAST) and the North Pacific Storm Track (NPST). In a warmer climate (i.e. $2\times\text{CO}_2$) one would expect (Geng & Sugi, 2001, 2003, Lambert, 1996, Schubert, 1998, Knipperitz et al., 2000, Carnell, 1996, 1998) the land-ocean temperature contrast to moderate especially during the winter months. Cold continental airmasses will not have as much punch on average due to the mean warmer climate. This creates a reduced thermal gradient on the eastern edges of the NH continents and could potentially reduce either the total number or intensity of cyclones or both in this ST region. Observational and modeling studies (Geng & Sugi, 2001, 2003, Lambert, 1996, Carnell, 1996) have more often than not shown a reduction in the total number of cyclones. The reduction of intensity is shown in some studies (Hall, 1994, Lunkeit, 1998, Carnell, 1996) and not in others (Lambert, 1996, Lim & Simmonds, 2003) depending on the latitude of interest. However there also is an extension of the NHST north and eastward especially in the eastern end of the NAST in a $2\times\text{CO}_2$ climate (Geng & Sugi, 2001, 2003, Sinclair, 1999, Schubert, 1998, Knipperitz et al., 2000).

Beyond the NHST, a very interesting component of a warmer climate is determining how and why the extreme event storms will evolve. It is these intense cyclones that create the largest anomalies in temperature and precipitation at the surface and invoke drastic changes to the entire tropospheric column. One would expect with a warmer climate that temperature gradients, environmental lapse rates, jet structures, and general circulation patterns to just name a few, would be significantly altered. ICEs are a small, unique but important subset of cyclones, through the analysis of which, a better understanding of the weather and climate changes in a warmer climate might be achieved.

This study compares the daily population of ICEs in the IPCC (Intergovernmental Panel on Climate Change) global warming scenario and a preindustrial control to determine how the population changes with a changing climate over the 20 year integrations for both experiments. The experiment chosen was the one percent annual increase in greenhouse gas emissions up to a level of $2\times\text{CO}_2$ of preindustrial conditions and from now on will be referred to as PCTTO2x. The control model run used for this analysis was the

preindustrial control (PreIndCtl). The GFDL_CM2.0 model which is one of the principal model members of the upcoming 4th Assessment Report (AR4) published by IPCC due to come out in 2007, is the model of choice for this study which utilizes the results of the aforementioned model runs.

The features of interest that will be the focused upon for these ICEs are the following: location/geographic distribution, occurrence during the year, and duration. Most importantly to this study is the climatology of the environment that the ICEs occur in during a global warming scenario and how this compares to a modern environment. If there are large phenomenological differences, the goal will be to determine how they manifest themselves in the ICEs. Making use of multivariable and multi-level dataset, a more complete picture will show in detail how ICEs will change in a global warming scenario.

The rest of this presentation is setup in the following manner. Section 2 explains the data used and the methods invoked to choose the ICEs. Section 3 will explain the changes in the temporal and spatial distributions of the ICEs, while Section 4 will investigate changes in model preferred months and regions that describe the ICE climatology. Finally a summary and conclusion in Section 5 will recap the major findings of this study.

2. DATA AND METHODOLOGY

The data for this study is based broadly upon the model output results from the GFDL_CM2.0 model, which is one of the ensemble members that will be used in the upcoming 4th Assessment Report (AR4) of Intergovernmental Panel on Climate Change (IPCC) due out in 2007. However, NCAR's CSM1.0 model (1997) was also examined to determine if the same type of intense cyclone trends were apparent in another model.

The specifics about the GFDL_CM2.0 model are as follows and are included in GFDL (2004). The GFDL_CM2.0 is a coupled climate model that includes atmosphere, ocean, land, and sea ice components. Fluxes are calculated for heat, moisture, and momentum within this model. The horizontal model resolution is 144x90 points or 2.5° longitude by 2.0° latitude. The vertical model resolution is based upon a hybrid coordinate grid that has 24 vertical levels that were interpolated to 17 standard pressure levels. The temporal resolution used in this analysis was daily mean data (24 hr) with a standard 365 day

(no leap) calendar. Twenty years of daily data were available from the control and transient experiments. However, to better emphasize Northern Hemispheric extratropical intense cyclone structure only a subset of the data was used. A six-month winter was used going from October 1 – March 31 (182 days) that captured 95% of the control and 96% of the experiment intense cyclone events. Also to ensure the chosen events were extratropical cyclones, only cyclones poleward of 20°N were examined. However, it should be noted that there were no intense cyclones that fit the criteria located south of 35°N. In addition, any cyclones that were close to the southern boundary that potentially could be tropical in nature were excluded. Nonetheless in both the control and experiment cases there were no such tropical occurrences.

The criteria that was used to define a Northern Hemisphere extratropical intense cyclone event (ICE) were the following: (1) the central sea-level pressure of the cyclone had to be less than or equal to 970 hPa; (2) The intense cyclone center had to exist for at least two consecutive time steps (24hrs) to be counted as an event; (3) To be called part of the same cyclone event, the intense cyclone center at a given time must have been within 20° latitude and 30° longitude of its previous location at the preceding time step; (4) The cyclone center had to be at or poleward of 20°N; (5) Lastly, there is no recognition of storm splitting or merging, each individual intense cyclone is perceived as an isolated event, without regard to any other cyclone activity (intense or not) at the same time step.

The preindustrial control climate simulation (PreIndCtl starting in 1860) is compared to the 1% annual increase of CO₂ until reaching CO₂ doubling experiment (PCTTO2x). The equilibrium climate sensitivity (ECS) of this experiment is 2.9K. The ECS is the difference between the experiment and the control global mean surface air temperature once they each are equilibrated individually. The purpose of choosing this particular experiment is to determine how, in a mean sense, intense cyclones vary in a warmer climate. The CO₂ doubling experiment also is a middle-of-the-road warming scenario as shown in Fig. 2.1. The PCTTO2x experiment used was the salmon colored line with solid end points from years 2061-2080 (model years 201-220). The PreIndCtl used was the aquamarine colored line with solid end points from years 1981-2000 (model years 121-140). Each IPCC model simulation may appear completely distinct despite similar forcings. However, the characteristics of this experiment

(PCTTO2x) may have some aspects that can be applied to the other IPCC scenarios and accompanying models that show the resultant inevitable warmer mean climate. Another focus of this study is to better understand not only the mean climate of a warmer world, but also in a day-to-day sense (synoptically). Will the storms that occur be more vigorous, more frequent, or farther reaching in extent (occurring in higher latitudes)? Most often climate studies look at monthly mean averages. This study is set apart by considering individual intense storms on the daily time scale, which demonstrates an important aspect of future weather that can be easily ignored or misrepresented by only examining the effects of the entire NHST.

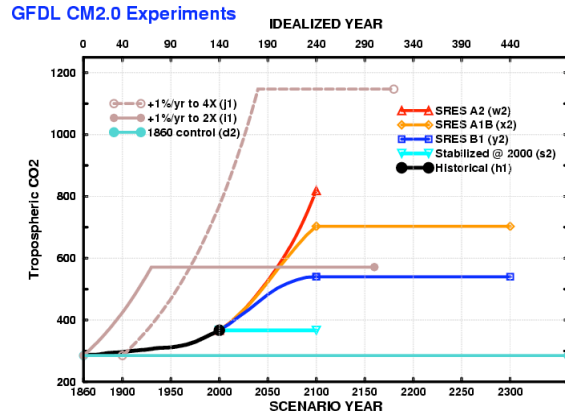


Fig. 2.1. Schematic of the time-varying atmospheric carbon dioxide levels specified in the various GFDL_CM2.0 experiments. It also depicts the initialization points used for the different experiments (GFDL Data Portal).*

3. ICE DISTRIBUTION

ICEs most often occur in preferred regions at certain times of the year. As might be expected by their extreme nature ICEs originate in regions with very large temperature gradients such as those that characterize the western boundary currents of the Gulf Stream and Kuroshio Current and extend into the North Atlantic and North Pacific Ocean basins, respectively. Also since mid-latitude cyclones derive their main energy source from strong temperature gradients, the boreal winter (and the months surrounding it), when the northern hemisphere has its largest mean baroclinicity, is the preferred season for the

* Schematic found on the GFDL data portal website at: http://nomads.gfdl.noaa.gov/CM2.X/CM2.0/data/cm2.0_data.html

ICEs. In this section the ICE distribution will be examined both temporally and spatially.

In order to examine the temporal distribution, we define an ICE day as any day within the 20-year model run (for either experiment) that includes a mid-latitude cyclone with a central sea-level pressure minimum below 970 hPa. Any given *model* day contains more than one ICE day if that day is characterized by multiple ICEs in different locations. Employing this definition, there were a total of 1603 and 1547 ICE days for the PCTTO2x and PreIndCtl experiments, respectively, representing a slight increase in the total number of ICE days (under 4%) from the PreIndCtl to the PCTTO2x experiment. This increase is not statistically significant since the difference does not exceed the 95% confidence interval, based on a two-tailed Student's t-test. All the ICE days were separated by month (not by events because some events span more than one month) as seen in Fig. 3.1 for both the PreIndCtl and PCTTO2x model runs. The obvious conclusion emerges that most ICE days occur between the months of October (month 10) and March (month 3) and from this point forward that period will be referred to as the 6-month winter (Oct.-Mar.). In fact, over 95% of all ICE days for both model runs occur within this 6-month winter time frame. There is no doubt that the months with the highest frequency of ICE days are December and January for both experiments. The next highest frequency months are November and February, followed by October and March. Each pair of these months has the latter winter month (January, February, and March) with more ICE days than its respective early winter month partner (December, November, and October) for the PreIndCtl. This trend reverses in the PCTTO2x experiment where there are more ICE days in the early winter month compared to the latter winter month for each pair. The increase in the number of ICE days in the early winter months and the decrease in the latter winter months in the PCTTO2x do not exceed the 95% confidence interval, according to the two-tailed Student's t-test. This result nonetheless suggests that the onset of the harshest part of the winter as measured by ICE days, comes slightly earlier in the PCTTO2x environment.

In Fig. 3.2 the duration of an individual ICE in days is compared to the number of ICEs that occur within the 20-year model run for each experiment. As expected, the shorter duration ICEs occur much more frequently than the longer duration ICEs. This is due mainly to the extreme

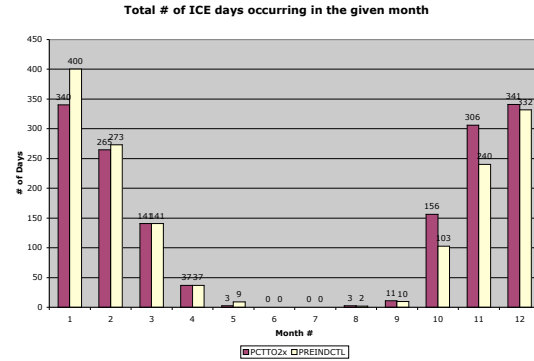


Fig. 3.1. Total number of ICE days that occur in the given numbered calendar month over 20-years of daily data for both the PCTTO2x (maroon) and the PreIndCtl (yellow).

nature of these events and how abnormal they are compared to the garden-variety cyclones. For ICEs occur much more frequently than the longer duration ICEs. This is due mainly to the extreme nature of these events and how abnormal they are compared to the garden-variety cyclones. For both experiments, an ICE day on average occurs once every 2 to 3 model days within the 6-month winter, which appears to be realistic according to modern observations (Martin, 2005). Figure 3.2 also shows that events longer than a week (7 days) in duration are extremely rare. When looking at events between 2 days and 7 days in duration, the PCTTO2x experiment has more events occurring than the PreIndCtl except at 2 and 7-day events. This result suggests that, in a global warming scenario, ICEs of longer duration would occur only slightly more frequently than their present-day counterparts.

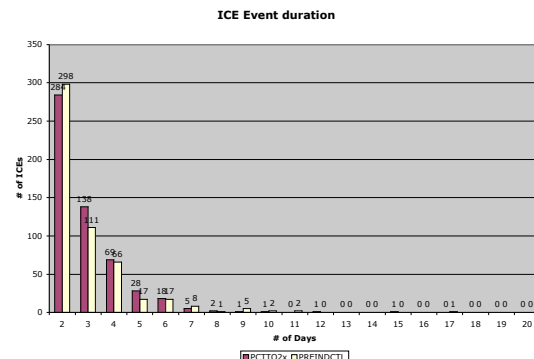


Fig. 3.2. The number of ICEs that occur for the given number of days of duration over 20-years of daily data for both the PCTTO2x (maroon) and the PreIndCtl (yellow).

Figure 3.3 shows the number of occurrences of ICE days in a given model year for

the PCTTO2x and PreIndCtl experiments. When looking between experiments there appears to be no systematic biased years and the number of ICE day occurrences seems to have the same relative scale (50-100+) despite the PCTTO2x experiment having slightly more ICE days overall. When dividing the 20-year dataset into the uppermost and lowermost quartiles (5 years of most/least occurrence each) there is a similar distribution between experiments. The upper quartile contains 33% and 31% of the occurrences in the PCTTO2x and PreIndCtl experiments, respectively, while the lowermost quartile contains 19% of the ICE days for both experiments. This leaves around 50% (48% in the PCTTO2x) of the ICE days to fall in the middle half of the data set.

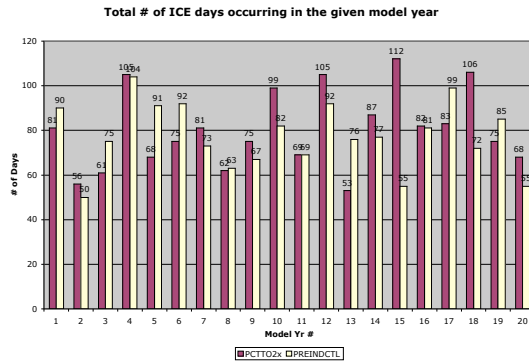


Fig. 3.3. Total number of ICE days that occur in the given numbered model year over 20-years of daily data for both the PCTTO2x (maroon) and the PreIndCtl (yellow).

The spatial distribution of the ICEs is also very important in understanding how the storm track potentially could change with a warmer climate. Figure 3.4 is a spatial density map (of 5° latitude x 5° longitude binned boxes) of the number of ICE days over the 20-year daily data set for both experiments. It is very apparent that the majority of the ICE days occur over the ocean basins, specifically the North Pacific and the North Atlantic. The density maxima in both experiments in the North Pacific is located in the vicinity of the southern Aleutian Islands which contains around 30 ICE days for the 20-year data set in both experiments. However, the ICE density maximum in the North Pacific (Bering Sea) in the PCTTO2x experiment is located approximately 10° longitude to the east at 52.5°N compared to the PreIndCtl. This eastward shift is consistent with an eastward extension of the NPST. Also in the region from 45°N-55°N and 155°E-155°W there is only one bin that does not exceed 14 ICE days in the PCTTO2x experiment. This same region has seven bins that

do not exceed 14 ICE days in the PreIndCtl. This suggests that the region including and surrounding the ICE density maximum in the North Pacific has a larger concentration of ICEs in the PCTTO2x experiment. In the North Atlantic the spatial density maxima is much reduced (~20 ICE days) and is located just southwest of Iceland for both experiments. The North Atlantic maximum is slightly more geographically spread out in the PreIndCtl.

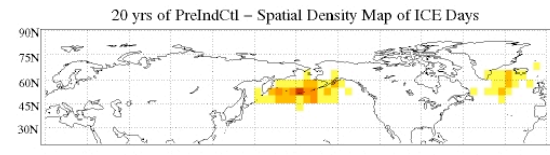
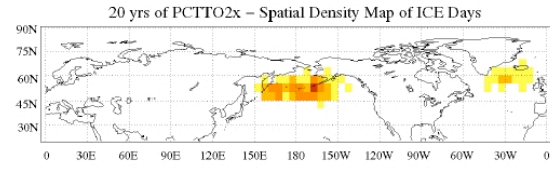


Fig. 3.4. (a) Spatial density map of the number of ICE days that occur over 20-years of daily data in the PCTTO2x for each 5° latitude by 5° longitude box. (b) As in Fig. 3.4a but for the PreIndCtl.

Figure 3.5 shows the locations of all the ICEs with their respective ICE days connected for each event. This view of the ICEs also confirms the aforementioned concentration of ICEs over the North Pacific and North Atlantic. A first order glance at all the ICEs suggests fairly similar distributions in the PCTTO2x and PreIndCtl experiments. It is also very noticeable there is a heavier concentration of ICEs in the North Pacific compared to the North Atlantic for both experiments.

The last set of spatially distributed ICE maps (Figs. 3.6-3.7) illustrates the ICEs that most frequently occur in the model months December and January. It should be noted that ICEs potentially could straddle model months (i.e. December and January). The ICE day's positions are only located on the map for the month in which they occur. So for example, a 3-day ICE that occurs from December 30-January 1 will have the position of all 3 ICE days, but will appear as a 2-

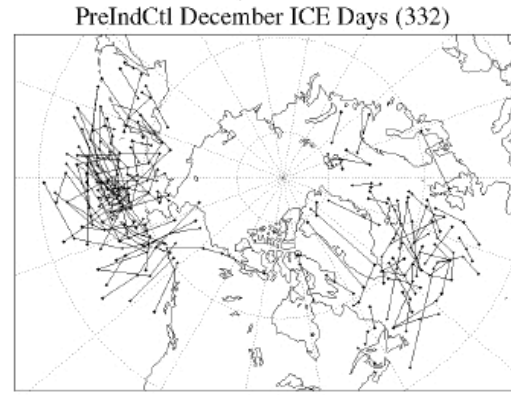
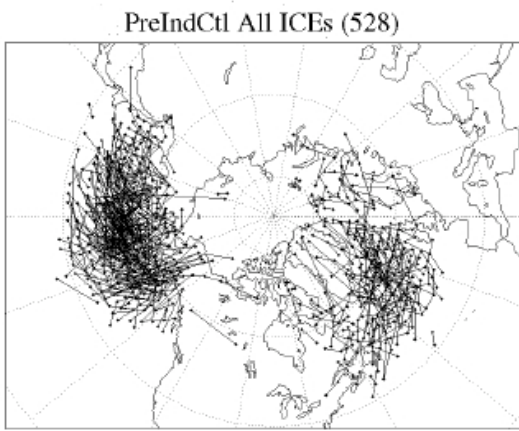
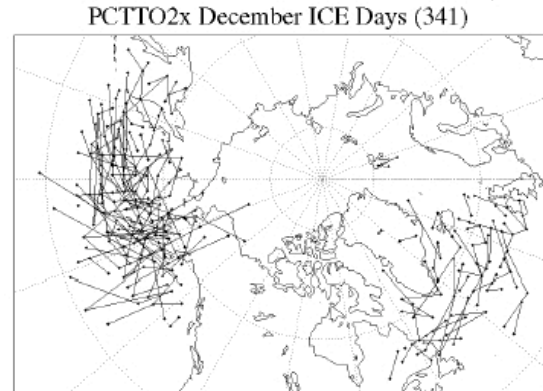
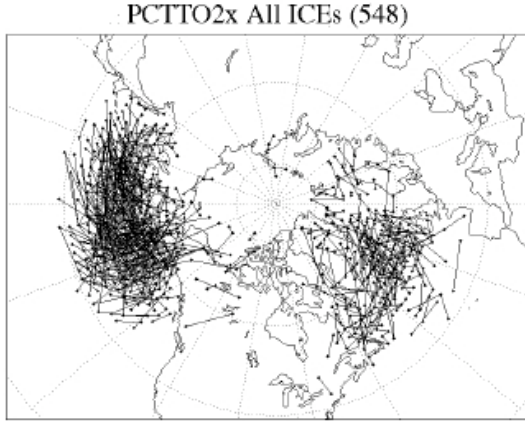


Fig. 3.5. (a) Spatial distribution map of all length duration ICEs over 20-years of daily data for the PCTTO2x (548 ICEs). (b) As in Fig. 3.5a except for the PreIndCtl (528 ICEs).

day event on the December map and a 1-day event on the January map even though it is a 3-day ICE event.

It is very noticeable that many more ICE days occur in the North Pacific basin compared to the North Atlantic for both experiments for both December and January. December ICE days (Fig. 3.6) show a larger number and longer duration of events in the PCTTO2x experiment in relation to the PreIndCtl. January (Fig. 3.7) reverses this trend by displaying more ICE days and longer duration ICEs in the PreIndCtl compared to the PCTTO2x.

Preferential ICE occurrences in space and time have been pointed out in this section. The location of the ICEs for all model times is over the ocean basins, specifically the North Pacific and North Atlantic. The seasonal occurrence of these ICEs is preferential to the NH cold season, centered on December and January but extending

Fig. 3.6. (a) Spatial distribution map of ICE days occurring in December over 20-years of daily data for the PCTTO2x (341 ICE days). (b) As in Fig. 3.6a except for the PreIndCtl (332 ICE days).

from October through March (6-month winter). Compared to the PreIndCtl, the PCTTO2x experiment appears to contain slightly more ICE days in October through December, slightly longer duration events, and a more concentrated distribution of ICE days in the North Pacific that is more eastward extending. Both experiments display more ICE days in the North Pacific compared to the North Atlantic and a similar occurrence distribution between model years. However, by and large, both model experiments seem to place the ICEs over nearly the same locations at the same time of year despite modest differences in total occurrences of ICEs and ICE days.

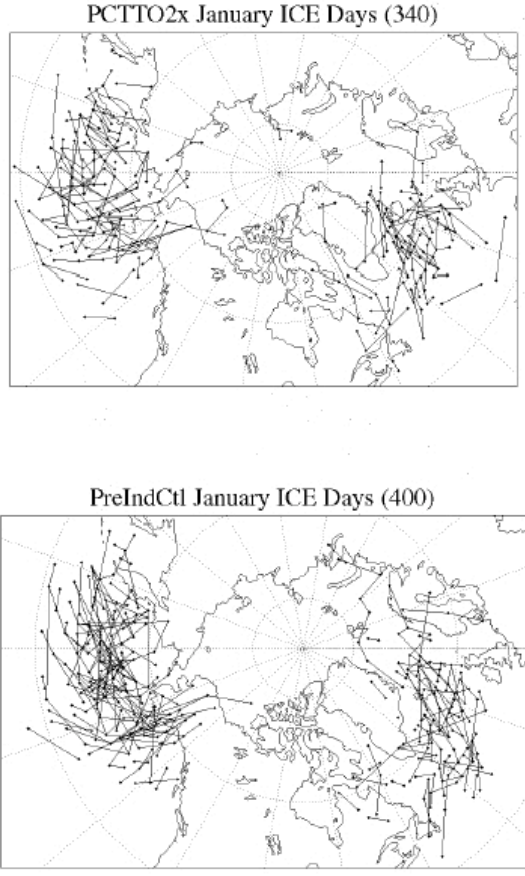


Fig. 3.7. (a) Spatial distribution map of ICE days occurring in January over 20-years of daily data for the PCTTO2x (340 ICE days). (b) As in Fig. 3.7a except for the PreIndCtl (400 ICE days).

4. Climatology

An understanding of the environment in which the ICEs form is vital to determining the important characteristics of these storms. Due to the extreme nature of the ICEs, it is certain that there must be some mid-level and upper-level dynamical support of the surface features. In this section the climatology of the hemisphere during the 6-month winter of the 20-year model run of both experiments at multiple vertical levels will be considered. Then an in-depth perspective of the atmospheric state during the model months of December and January for both experiments will be examined. Throughout this section the similarities and differences between the PCTTO2x and PreIndCtl experiments will be highlighted.

Figures 4.1-4.3 in this section are three panel figures. Panel “a” on each represents the quantity of interest from the PCTTO2x experiment, Panel “b” represents the quantity of interest from PreIndCtl experiment, and Panel “c” will be the

difference field (PCTTO2x-PreIndCtl) of that quantity between the two simulations. The NH 20-year daily averaged 6-month winter is displayed in Figs. 4.1-4.2 at the 300 hPa and 500 hPa levels. For this pair of figures isotachs are shaded and geopotential heights are contoured at the specified levels. The jet cores at both 300 hPa and 500 hPa are located just off the east coasts of North America and Asia between latitudes 25°N and 50°N for both experiments.

Figure 4.1 shows a very similar picture in the jet structure for both experiments at 300 hPa. The only differences seen in Fig. 4.1c are wind speed differences less than 4 m/s over south central Asia, northwestern China and northern Japan, and in the central and eastern North Pacific. The slight increase of wind speed over the central Pacific is the result of a slight northeastward extension of the climatological jet in the PCTTO2x experiment. The geopotential height field at this level has the same general structure between the two experiments as seen in Figs. 4.1a and 4.1b. The major differences between these figures once again are shown in Fig. 4.1c, which depicts modest height rises across the entire hemisphere in the PCTTO2x experiment. These height rises associated with higher thicknesses from 1000 hPa–300 hPa would be consistent with a warmer climate and represent the thermal structure in the upper troposphere to support it. A fairly large height increase of ~300 meters is seen in the Barents Sea region north of western Russia in the PCTTO2x experiment. This is thought to reflect the much warmer atmosphere over the Barents Sea in the PCTTO2x environment resulting from decreased sea ice cover in this region.

Figure 4.2 illustrates the geopotential height and isotachs at 500 hPa over the NH for the daily mean climatology over the 20-year period for the 6-month winter for both experiments. The jet cores at 500 hPa are virtually co-located with those at 300 hPa just off the North American east coast and the Asian east coast. Figure 4.2c depicts minimal increases in the wind speeds (< 2 m/s) over the entire hemisphere, which are negligible. Also similar to the 300 hPa maps, there are geopotential height increases everywhere, which is again indicative of the warmer climate in the PCTTO2x experiment. These height rises are fairly modest except in one location, the Barents Sea region which shows a height increase around 180 meters. The constant appearance of a large height anomaly over the Barents Sea is an important localized feature that is, again, related to

a large reduction of sea ice over the time period of interest.

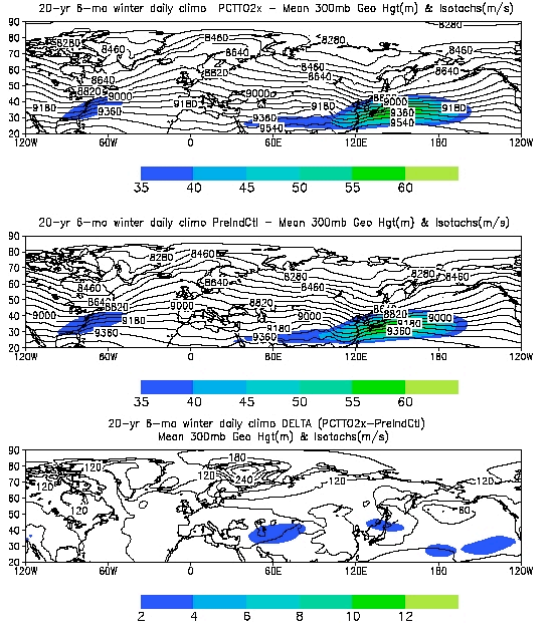


Fig. 4.1. (a) PCTTO2x 20-year 6-month winter mean daily 300 hPa geopotential height (solid lines) labeled in m contoured every 90m and isotachs (shaded) in m/s and shaded every 5 m/s beginning at 35 m/s. (b) As for Fig. 4.1a except for the PreIndCtl experiment. (c) As for Fig. 4.1a except for the difference between the experiments (PCTTO2x-PreIndCtl), the geopotential height is contoured every 60m, and the isotachs are shaded every 2 m/s beginning at 2 m/s.

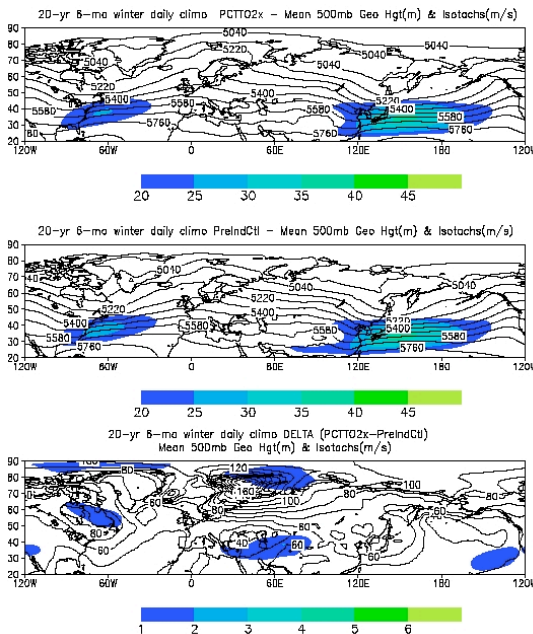


Fig. 4.2. (a) PCTTO2x 20-year 6-month winter mean daily 500 hPa geopotential height (solid lines) labeled in

m contoured every 90m and isotachs (shaded) in m/s and shaded every 5 m/s beginning at 20 m/s. (b) As for Fig. 4.2a except for the PreIndCtl experiment. (c) As for Fig. 4.2a except for the difference between the experiments (PCTTO2x-PreIndCtl), the geopotential height is contoured every 10m, and the isotachs are shaded every 2 m/s beginning at 1 m/s.

Another key component in understanding the climatology of NH extratropical cyclones is appreciating the relationship between surface pressure and the lower tropospheric thermal structure. This relationship is manifested in Fig. 4.3 for both experiments by looking at the mean sea-level pressure (shaded) and 1000 hPa-500 hPa thickness fields (solid lines). Both experiments show the climatological low pressure systems better known as the Icelandic Low and the Aleutian Low. Also a high pressure area is consistently centered over the Himalayas in Asia. The difference plot (Fig. 4.3c) between the PCTTO2x and the PreIndCtl will be referred to for determining changes in the PSL and thickness fields. In this figure the weakly enhanced Azores High over the North Atlantic and Europe coupled with an enhanced Icelandic Low to its north extending its lowered PSL westward to Greenland and eastward into the Arctic Ocean over central Russia would produce an enhanced positive phase of the North Atlantic Oscillation (NAO) in the PSL field for the PCTTO2x environment. Another dipole in the PSL field that appears is the one located over the North Pacific. The region of higher sea-level pressures from eastern China to south of Japan and lower sea-level pressures over the Aleutian Islands is not indicative of any one low frequency NH teleconnection pattern but more than likely is a combination of several patterns. In addition, the thermal field, represented by the 1000 hPa – 500 hPa thickness, displays its largest changes in the PCTTO2x experiment almost exclusively over the Barents Sea. So collectively, both the Aleutian and Icelandic lows are deeper and stronger in the PCTTO2x experiment. Also of note, there is weaker warm front baroclinicity as seen in a poleward increasing thickness difference along the Aleutian Islands despite a stronger Aleutian low.

An additional useful aspect to analyze when investigating changes in the PCTTO2x environment is vertical cross-sections of the wind, specific humidity, and temperature. Diagnosing the zonally averaged, time averaged fields of the wind components (u , v), specific humidity, and temperature is accomplished in Figs. 4.4-4.7, respectively. Figure 4.4 depicts the u -component of the upper-tropospheric jet centered over 30°N

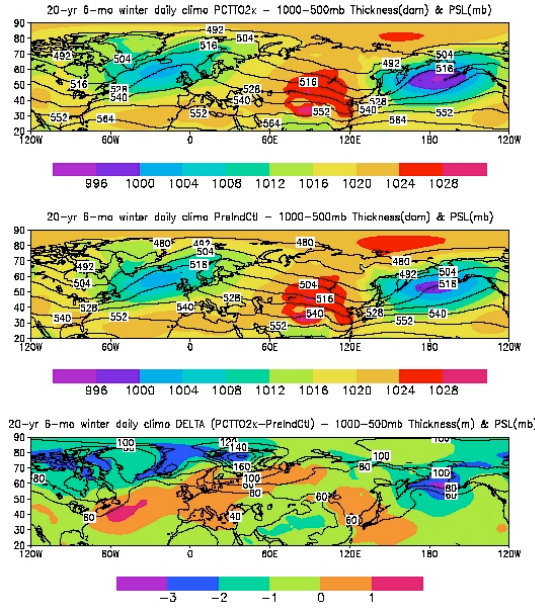


Fig. 4.3. (a) PCTTO2x 20-year 6-month winter mean daily 1000-500 hPa thickness (solid lines) labeled in dam contoured every 12dam and sea-level pressure (shaded) in mb and shaded every 4 mb beginning at 996 mb. (b) As for Fig. 4.3a except for the PreIndCtl experiment. (c) As for Fig. 4.3a except for the difference between the experiments (PCTTO2x-PreIndCtl), the 1000-500 hPa thickness is contoured every 20m, and the sea-level pressure is shaded every 1 mb beginning at -3 mb.

around 40 m/s with decreasing values of the *u*-component of the wind elsewhere (poleward and closer to the surface) for both experiments (Figs. 4.4a and 4.4b). Figure 4.4c shows the differences in the zonally averaged *u*-component of the wind between the experiments. This figure shows a tripole structure of this variable in the mid and upper levels of the atmosphere. It shows an increase in the *u*-component around 250mb at 40°N flanked by decreases around 20°N at 500mb and 60°N at 400mb. This structure is indicative of the upper-level jet shifting northward. It also leads to enhanced upper-level cyclonic vorticity around 50°N and anticyclonic vorticity around 30°N. The consequence of the upper-level vorticity difference couplet would be consistent with a northward shift of the storm track, which occurs on the northeast flank of the NAST and NPST. Changes in the low-level *u*-component of the wind in the warmer environment seem virtually inconsequential.

The *v*-component of the mean wind that is shown in Fig. 4.5 is a partial estimation for the meridional heat and moisture transport (fluxes by transients are also very important which are not shown). For both experiments (Fig. 4.5a and 4.5b), the

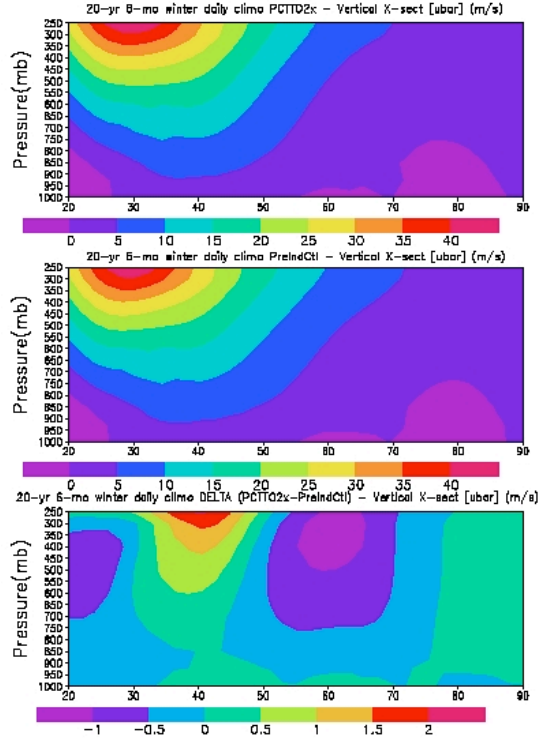


Fig. 4.4. (a) PCTTO2x 20-year 6-month winter mean daily vertical cross-section of zonally averaged *u*-component of the wind (shaded) labeled in m/s and shaded every 5 m/s beginning at 0 m/s. (b) As for Fig. 4.4a except for the PreIndCtl experiment. (c) As for Fig. 4.4a except for the difference between the experiments (PCTTO2x-PreIndCtl) and the zonally averaged *u*-component of the wind is shaded every 0.5 m/s beginning at -1 m/s.

northern extension of the Hadley cell appears as equatorward flow (negative *v*-component values) near the surface between 20°N-30°N and poleward flow (positive *v*-component values) in the upper-atmosphere at these same latitudes. The other prominent feature that appears for both experiments is the upper equatorward branch of the Ferrel cell centered on 50°N. When looking at the differences between the two experiments (Fig. 4.5c) there really are only changes in the *v*-component of the wind at high latitudes (70°N-90°N) with an increase at the surface and decrease at upper-levels, which would weaken the polar cell. Through the meridional advection influence, one can argue that there will be a warming at the surface and cooling at upper-levels, which would reduce the static stability at these high latitudes. It should be noted that the northern most latitude in the model simulations is 87.5°N and any apparent transport through the North Pole is a figment of the model grid spacing.

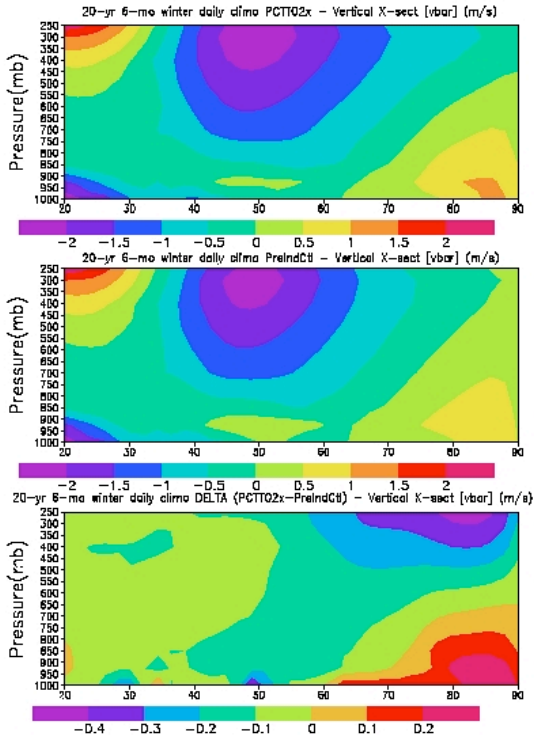


Fig. 4.5. (a) PCTTO2x 20-year 6-month winter mean daily vertical cross-section of zonally averaged v-component of the wind (shaded) labeled in m/s and shaded every 0.5 m/s beginning at -2 m/s. (b) As for Fig. 4.5a except for the PreIndCtl experiment. (c) As for Fig. 4.5a except for the difference between the experiments (PCTTO2x-PreIndCtl) and the zonally averaged v-component of the wind is shaded every 0.1 m/s beginning at -0.4 m/s.

Figure 4.6 depicts a vertical cross-section of the zonally and temporally averaged specific humidity in the atmosphere for both experiments (Fig. 4.6a and 4.6b) and the difference between them (Fig. 4.6c) shown as a percentage change. Lower altitudes and latitudes have the largest values of specific humidity for both experiments due to the relatively warmer temperatures in these regions. It is undetermined if changes in actual moisture content or the relative amount of moisture in the atmosphere are more pertinent to changes in cyclone development. Despite this, it is intriguing to look at the percentage increase in the specific humidity, which appears to be at similar latitudes with the largest increases in ICEs. The percentage increases in moisture (specific humidity shown Fig. 4.6c) in the atmosphere would be concentrated at high latitudes and low elevations in the atmosphere in the PCTTO2x experiment. The regionally enhanced poleward heat and moisture flux in the PCTTO2x experiment is potentially the result of the slight

increase of ICEs in the high latitudes. This also could be accomplished by polar amplification. Nonetheless, both certainly would seem to positively feedback on warmer, moister high latitudes in a global warming scenario.

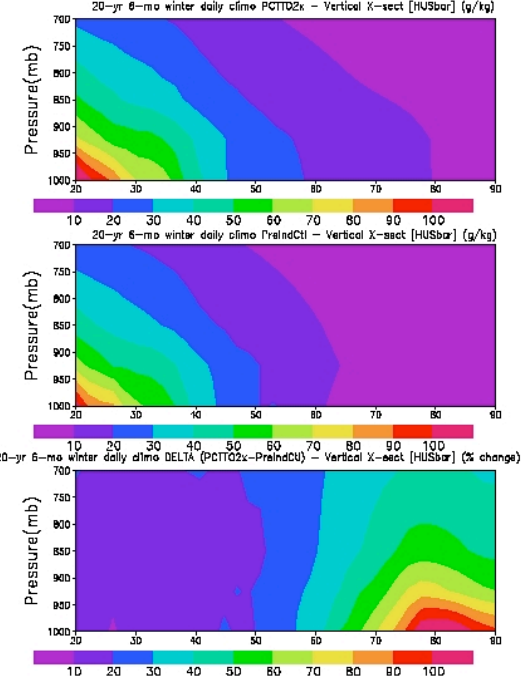


Fig. 4.6. (a) PCTTO2x 20-year 6-month winter mean daily vertical cross-section of zonally averaged specific humidity (shaded) labeled in g/kg and shaded every 10 g/kg beginning at 10 g/kg. (b) As for Fig. 4.6a except for the PreIndCtl experiment. (c) As for Fig. 4.6a except for the difference between the experiments (PCTTO2x-PreIndCtl) and the zonally averaged specific humidity is shown as a percentage change.

The vertical cross-section of zonally and temporally averaged temperature is shown in Fig. 4.7 for both experiments. As expected, warmer temperatures are seen equatorward and towards the surface for both experiments (Figs. 4.7a and 4.7b). The difference in temperature between these experiments is observed in Fig. 4.8c where increases in temperature are seen at all levels (1000mb-250mb) and latitudes (20°N-90°N) in the PCTTO2x experiment. However, large localized temperature increases ($\geq 4^{\circ}\text{C}$) are realized from 55°N-90°N in the 200 hPa closest to the surface. This region of the atmosphere would account for the largest changes in the low-level temperature gradients. Since this warming occurs at higher latitudes, where there is a heat deficit, a relaxation of the pole-to-equator temperature gradient results, reducing the large-scale low-level baroclinicity. Outside of this region (lower

latitudes in the NH and mid and upper levels of the atmosphere), there seems to be little change in the temperature field in the PCTTO2x except for a general warming. This would mean little change in the hemispheric temperature gradients and thus baroclinicity outside of the aforementioned low-level, higher latitude region. This slightly weakened baroclinicity, especially at NHST latitudes (30°N - 60°N), would logically lead to the assumption of a small decrease in the development of extratropical cyclones. This experiment was not tested, nor was the focus of this study, but seems consistent with other model experiments (Carnell, 1996, 1998, Hall, 1994, Lunkeit, 1998, etc.) that have been performed and theories of cyclogenesis.

The globally averaged increase in temperature in the PCTTO2x experiment does not imply a change in the meridional temperature gradient. Figure 4.7c convincingly shows no significant change in the baroclinicity from about 800 hPa – 400 hPa (and none from 600 hPa – 400 hPa) throughout the NH in the PCTTO2x environment. Surface cyclone development is largely controlled by geostrophic vorticity advection by the thermal wind (Sutcliffe 1947). Since neither the vertical shear nor the mid-tropospheric geostrophic vorticity appear to show much change in a doubled CO_2 environment, there is little reason to expect significant changes in the basic forcing mechanism. This means that baroclinic energy conversion should be largely unaffected in the PCTTO2x environment.

As determined in the last section, ICEs preferentially occur during the boreal winter. More specifically, the peak of the ICE season is during the calendar months of December and January. To achieve further insight about some of the more intricate differences between the PreIndCtl and the PCTTO2x experiments, a detailed analysis of the months of December and January is performed. Also a polar stereographic view is adopted to get a more complete hemispheric outlook of each experiment.

Figure 4.8 shows the changes in the PCTTO2x environment for the daily averaged December at various levels of the atmosphere for multiple variables. Figure 4.8a depicts wind increases around 2-6 m/s centered between 30°N - 40°N at 300 hPa. However, the largest geopotential height increases at the same level are located at much higher latitudes (55°N - 80°N) implying the height differences are distinct from the wind increases. Nonetheless the height increases would imply much warmer temperatures

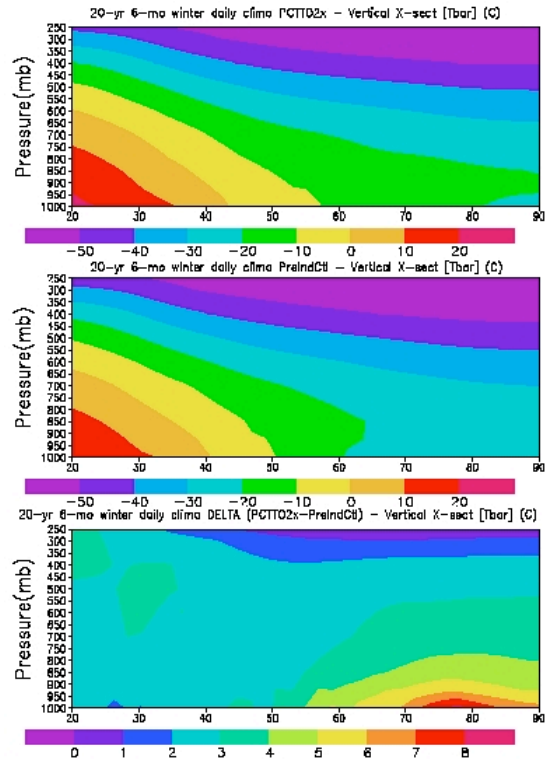


Fig. 4.7. (a) PCTTO2x 20-year 6-month winter mean daily vertical cross-section of zonally averaged temperature (shaded) labeled in $^{\circ}\text{C}$ and shaded every 10°C beginning at -50°C . (b) As for Fig. 4.7a except for the PreIndCtl experiment. (c) As for Fig. 4.7a except for the difference between the experiments (PCTTO2x-PreIndCtl) and the zonally averaged temperature is shaded every 1°C beginning at 0°C .

most likely in the lower troposphere at high latitudes in the PCTTO2x experiment (as seen in Fig. 4.8c) during December. Figure 4.8b illustrates the differences in the winds and geopotential heights at 500 hPa between the experiments in December. The locations with the wind increases and height increases at 500 hPa are separate, and nearly are co-located with those at the 300 hPa level. In addition to the wind speed increases between 30°N - 40°N , there is a slight increase in wind speed over the Gulf of Alaska by 2-3 m/s much like at 300 hPa.

It is also not a coincidence that there are similar wind speed increases at 300 hPa and deepened sea-level pressure minima at the surface (Fig. 4.8c) over the same locations. Figure 4.8c displays sea level pressure and 1000hPa-500hPa thickness differences between the PCTTO2x and PreIndCtl experiments for the daily averaged December. There are sea-level pressure decreases over the Bering Sea and the central North Pacific, while there are large

increases over the East Siberian Sea and eastern Siberia and also to a lesser degree over central Europe. Thickness increases are seen over the entire hemisphere with the largest increase over the Barents Sea. There also is a prominent thickness gradient over the Bering Sea with larger thickness differences to the north. Since the thermal wind blows parallel to the thickness contours and its magnitude is inversely proportional to the spacing between the contours, it is conceivable to imagine a decrease in cold-air surges exiting the Asian continent (over eastern Siberia) and being advected back over Eastern Siberia. In addition, the vertical shear profile suggests strong northeasterly flow over the Bering Sea, which can only be indicative of an extremely occluded or equivalent barotropic cyclone structure in the mean difference field, not a developing ICE to the extent that the mean structure represents the ICE structure. However, to maintain approximately the same number (slight increase) of ICEs without baroclinic instability, there must be an alternative developmental mechanism. A probable candidate for this task is a diabatic effect, which more than likely is an increased latent heat flux from the ocean to the atmosphere that is forced by replacing sea ice in this region with open water (Vavrus, 2005). This phase change reduces the albedo of the surface and dissolves the capping of the relatively warmer ocean water that was in place with the sea ice.

To further analyze how December in the PCTTO2x is different than January, vertical cross-sections are examined in Fig. 4.9. Figures 4.9a and 4.9b show the differences in the u and v components of the wind respectively while Fig. 4.9c depicts differences in temperature between the experiments during the daily averaged December. The predominate feature of interest in Fig. 4.9a is the couplet of increased and decreased westerly winds near the tropopause pivoted around 50°N . The increased westerly winds around 40°N and increased easterly winds around 60°N are conducive to more cyclonic vorticity at upper-levels near 50°N . This in part, is consistent with a shift of the storm track to slightly higher latitudes. Figure 4.9b demonstrates at very high latitudes (70°N - 90°N) much increased poleward heat and moisture transport at low levels while increased equatorward transport at upper levels. This induced circulation near the North Pole implies an anomalous poleward heat and moisture transport that could develop and sustain extratropical cyclones at very high latitudes, which are not that common in the PreIndCtl. Figure 4.9c reveals zonally averaged, daily averaged,

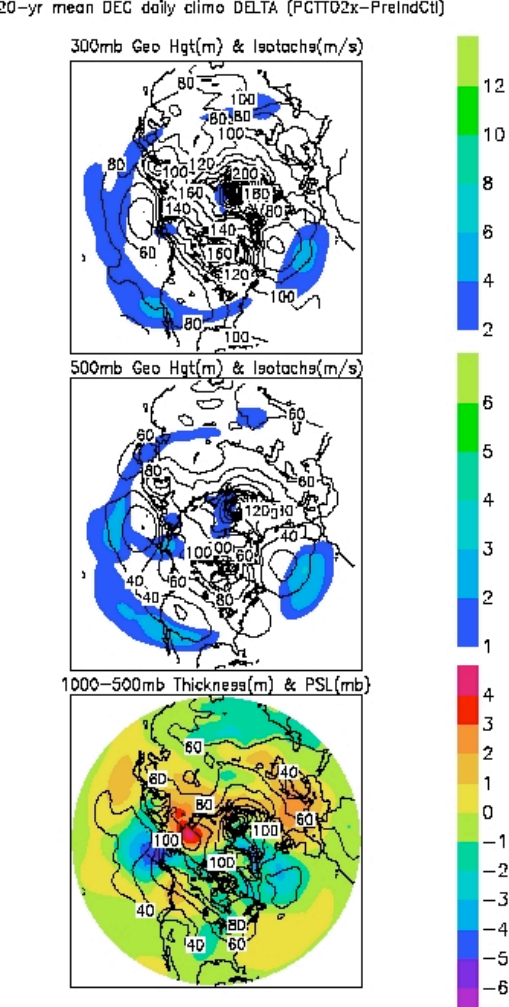


Fig. 4.8. (a) Difference between the experiments (PCTTO2x-PreIndCtl) 20-year December mean daily 300 hPa geopotential height (solid lines) labeled in m contoured every 20m and isotachs (shaded) in m/s and shaded every 2 m/s beginning at 2 m/s. (b) As for Fig. 4.8a except at the 500 hPa level and the isotachs are shaded every 1 m/s beginning at 1 m/s. (c) As for Fig. 4.8a except 1000-500 thickness (solid lines) is labeled in m contoured every 20m and the sea-level pressure is shaded every 1 mb beginning at -6 mb.

temperature changes between the experiments in December. As suspected, the largest temperature changes occur in high latitudes of the NH with maximum increases around 8°C between 75°N - 82°N at the surface. Since these high latitudes are largely ocean or sea ice during the winter months, this polar amplification of temperature increases is due mainly to the altered ocean-atmosphere heat flux, which was nearly non-existent at the very high latitudes during December in the PreIndCtl and is much increased in the PCTTO2x.

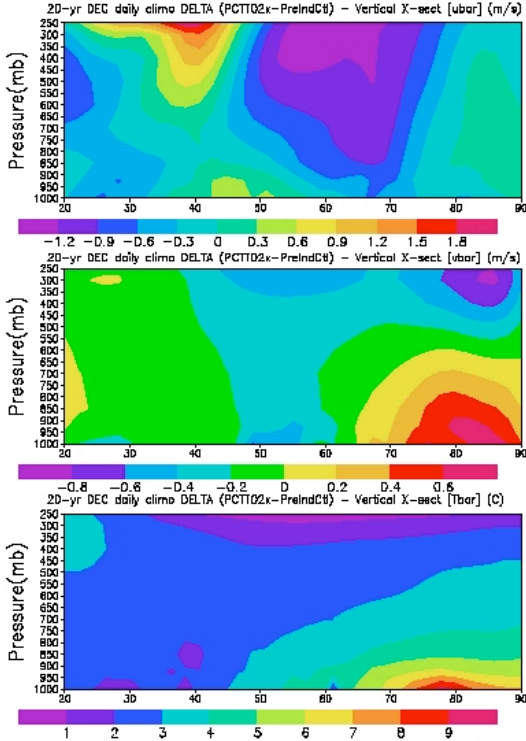


Fig. 4.9. (a) Difference between the experiments (PCTTO2x-PreIndCtl) 20-year December mean daily vertical cross-section of the zonally averaged u -component of the wind (shaded) labeled in m/s and shaded every 0.3 m/s beginning at -1.2 m/s. (b) As for Fig. 4.9a except for the zonally averaged v -component of the wind is shaded every 0.2 m/s beginning at -0.8 m/s. (c) As for Fig. 4.9a except for the zonally averaged temperature is labeled in $^{\circ}$ C and shaded every 1 $^{\circ}$ C beginning at 1 $^{\circ}$ C.

Figure 4.10 shows the changes in the PCTTO2x environment for the daily averaged January at 300 hPa, 500 hPa, and the surface (\sim 1000 hPa). One result of the changes in January in the PCTTO2x experiment was a pronounced decrease in the number of ICE days (400 down to 340) from the PreIndCtl. Increases in the wind speed and the geopotential height at 300 hPa are depicted in Fig. 4.10a. Wind speed increases cover a larger geographical area and have larger magnitudes in some regions (around 6-8 m/s in the Arctic Ocean north of central Russia) in January than they do in December. There also is geopotential height rises over the entire hemisphere much like in December. There are three focused regions for these height rises, the Barents Sea, Hudson Bay, and eastern Siberia/Bering Sea. At 500 hPa (Fig. 4.10b) the regions of increased wind speeds and geopotential height are located in general agreement with those at 300 hPa, however, with

decreased magnitude of wind speed increases and heights. Figure 4.10c illustrates temperature increases in the low atmosphere (1000 hPa-500 hPa thickness) over the entire hemisphere and concentrated increases over the same three regions seen in the height fields at 300 hPa and 500 hPa. The sea-level pressure field has quite a different pattern in January compared to that in December. The only region with a large decrease in the sea-level pressure field is over much of Siberia. Otherwise there are large sea-level rises over the Gulf of Alaska, Western Europe, and the Norwegian Sea. This pattern would be indicative of a large decrease in cyclones over the North Atlantic and a westward shift of the Aleutian Low, which is reflected, to some degree in Fig. 3.7.

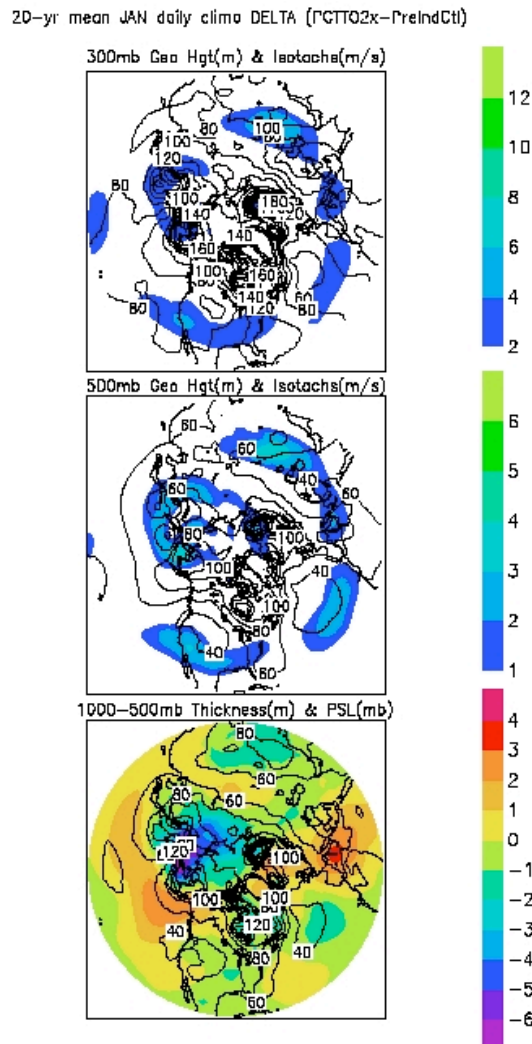


Fig. 4.10. (a) Difference between the experiments (PCTTO2x-PreIndCtl) 20-year January mean daily 300 hPa geopotential height (solid lines) labeled in m contoured every 20m and isotachs (shaded) in m/s and shaded every 2 m/s beginning at 2 m/s. (b) As for Fig.

4.10a except at the 500 hPa level and the isotachs are shaded every 1 m/s beginning at 1 m/s. (c) As for Fig. 4.10a except 1000-500 thickness (solid lines) is labeled in m contoured every 20m and the sea-level pressure is shaded every 1 mb beginning at -6 mb.

Vertical cross-sections as shown in Fig. 4.11 are another key element in understanding the decrease in ICE days in the PCTTO2x experiment in January. The zonally and time averaged u -component of the wind is described in Fig. 4.11a. There is a couplet of increased mid- and upper-level easterly winds from 20°N - 30°N and increased westerly winds from 30°N - 50°N . The increased easterly winds are on the southern flank of the increased westerly jet in January compared to on the northern flank in December. This couplet is conducive to an enhanced anticyclonic circulation centered on 30°N , which obviously inhibits cyclone formation at upper-levels. The v -component of the wind is depicted in Fig. 4.11b. This diagram implies a much different picture of the changes in heat and moisture transport accomplished by the mean meridional circulation compared to December. The largest poleward transport is near the surface from 35°N - 60°N , while the largest equatorward transport is located at upper levels between 25°N - 45°N with another region near the surface and aloft between 60°N - 80°N . This pattern is not indicative of concentrated increased poleward temperature amplification. Nonetheless, significant increases in high latitude, lower troposphere temperatures are seen in Fig. 4.11c. There is a spreading out of the large temperature increases at the surface from 50°N - 90°N . More of the increase in temperature in January would be due to the sea-ice being replaced by open ocean compared to an enhancement of poleward heat transport by the atmosphere and/or ocean as in December. All these constituents factor into the reduced number of ICE days during January in the PCTTO2x experiment. At the current time, the author is unaware of any literature that either has broken down the changes in a doubled CO_2 environment by month (only seen done by season) or has tried to explain the physical differences between these months (December and January) in a warmer climate.

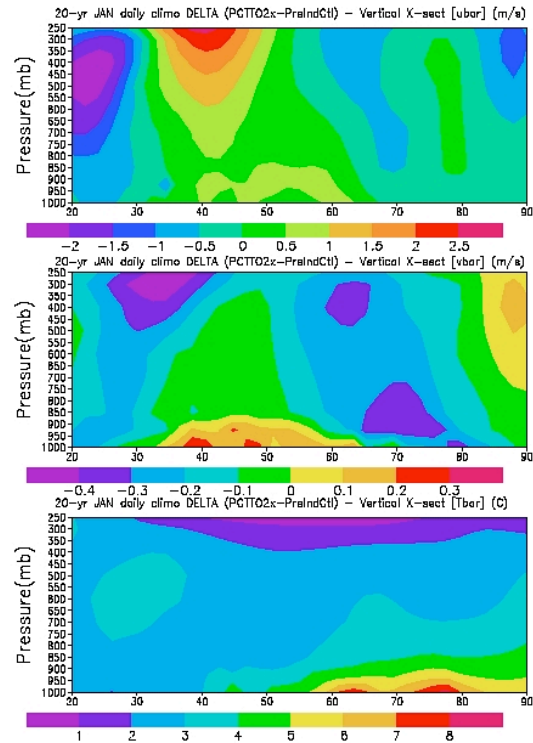


Fig. 4.11. (a) Difference between the experiments (PCTTO2x-PreIndCtl) 20-year January mean daily vertical cross-section of the zonally averaged u -component of the wind (shaded) labeled in m/s and shaded every 0.3 m/s beginning at -1.2 m/s. (b) As for Fig. 4.11a except for the zonally averaged v -component of the wind is shaded every 0.2 m/s beginning at -0.8 m/s. (c) As for Fig. 4.11a except for the zonally averaged temperature is labeled in $^{\circ}\text{C}$ and shaded every 1°C beginning at 1°C .

5. Summary and Conclusion

Many of the global warming mean climate differences that were noted in other climate change studies were born out in this study. One of the most apparent results of the PCTTO2x environment was that global warming throughout the NH inherently decreased the low level pole-to-equator temperature gradient. The reduction of the meridional temperature gradient directly correlates to a reduction in the large-scale hemispheric meridional baroclinicity, which is the main energy source used by NH extratropical cyclones for intensification. Such a circumstance might lead to the expectation that the total number or the intensity of the majority of NH extratropical cyclones would decrease. As it turns out through this analysis, by and large, the total number and distribution of ICEs are not very different between the PreIndCtl and the PCTTO2x in the GFDL_CM2.0 model. Nonetheless, it is quite

possible that the population of extratropical cyclones will be significantly effected and that such differences may manifest themselves as changes in frequency, ferocity, and/or developmental mechanism.

Despite a lot of attention directed towards the state of the mean climate in a doubled CO₂ environment there has been little discussion in the literature of the effects this warmer climate will have on the strongest NH extratropical storms. This has motivated an in-depth examination of changes to “intense cyclone events” (ICEs) in a global warming scenario. ICEs were defined as NH extratropical cyclones whose central pressure was 970 hPa or less for at least 24 hours. Comparisons of twenty-year climatologies of the synoptic environment in which these ICEs form, from 20°N to 90°N, for the PCTTO2x and PreIndCtl experiments was the basis for this study. The temporal frequency of the ICEs highly favored occurrence (95% of all ICEs for both experiments) during the boreal winter months and those months directly surrounding it (October-March), which were termed the “6 month winter.” The most frequent calendar months specifically were December and January. The spatial distribution of the ICEs were firmly anchored in the NH ocean basins originating over the western boundary currents, the Gulf Stream and the Kuroshio Current, of the North Atlantic and North Pacific, respectively. There were significantly more ICEs in the Pacific than in Atlantic for virtually all duration events and months. Shorter duration (2-3 day) events were by far the most common ICEs.

There are also some trends that should be noted that occur in the PCTTO2x experiment. There is a seasonal shift of ICEs occurring most frequently from the latter part of the cold season (January-March) to the early part of the cold season (October-December). The ICE duration becomes slightly longer in the PCTTO2x experiment. Both of these trends, though interesting, are not statistically significant according to the 95% confidence interval, based upon the Student’s t-test. Also, the total number of ICE days occurring in a given model year for either experiment did not show a trend from year to year. Most years showed similar high and low counts of ICE days for both experiments. Changes between the PCTTO2x and PreIndCtl ICEs are similar to those seen in the current climate between years or different subsets of the dataset (not shown). Therefore the changes in the doubled CO₂ environment are not necessarily “unique” to occurrence in the PCTTO2x environment.

The average synoptic environment in which the ICEs developed was fairly similar for both experiments. The mean sea-level pressure across the NH from 20°N-90°N decreased by nearly half a millibar (1017.21 mb in the PreIndCtl down to 1016.73mb in the PCTTO2x). Sea-level pressure is a measure of the weight of the atmosphere above the surface and the model has an arbitrary top of the atmosphere (TOA). This would mean that the weight of the model atmospheric column (surface to TOA) is slightly lighter in the PCTTO2x experiment. Since warm air is less dense than cooler air, this drop in sea-level pressure due to this column is consistent with a warmer climate (atmosphere) in this model simulation. The standard deviation of sea-level pressure from 20°N-90°N varies little from the PCTTO2x to the PreIndCtl (9.60mb compared to 9.65mb). There also is little difference when calculating one standard deviation of sea-level pressure over the ST region (30°N-60°N), which only varies from 10.45mb in the PCTTO2x to 10.44mb in the PreIndCtl. The ICE population and the mean PSL for both experiments were very similar, thus the threshold value of 970 hPa for ICEs is approximately 5 standard deviations (4.87 in the PCTTO2x and 4.89 in the PreIndCtl) below the mean PSL in each experiment. All of these climatological statistics lead to the speculation that the global mean climates portrayed in each experiment in the GFDL_CM2.0 model are very similar despite the PCTTO2x simulation being slightly warmer.

Globally the climate change is small, however regionally the differences are much greater. Strengthened regional poleward heat and moisture transport in the ocean and atmosphere in the PCTTO2x experiment accompanied with land-sea differences leads to an uneven distribution of these variables throughout the hemisphere; thus some regions show a strong signal of polar amplification while other regions only slightly change. The largest changes in heat and moisture due to a doubled CO₂ environment are largely near the surface over the NHST and slightly poleward. Both portions of the NHST, the NAST and the NPST, show a northward shift accompanied by an eastward extension particularly over the NPST in the PCTTO2x experiment. Associated with the reduction in the NH pole-to-equator temperature gradient at the surface, there would be a reduction in the low level static stability on the south side of the polar front, thereby allowing for an enhancement of vertical mixing at these latitudes. In addition, there is a slight intensification of the temperature gradient at

upper levels especially at high latitudes in the atmosphere. One likely outcome of this finding would be more storms that occur at higher latitudes and originating at higher altitudes than those in the PreIndCtl. Thus vertical coupling to upper level features may be even more important in the PCTTO2x experiment than in the PreIndCtl environment.

Changes in the actual number of ICEs and number of ICE days increased by 4% (both are not statistically significant) in the PCTTO2x experiment. Nonetheless, this result is one of the major findings of this study. There is an increase in intense storms, but only slightly. There are undoubtedly multiple changes occurring in the PCTTO2x experiment. The decreased hemispheric temperature gradient in part is offset by the northward shift of the ST and the enhanced cyclone coupling to the upper levels. The other, largely contributing component to changes in ICEs has been theorized by past literature as being the increase in moisture content in the atmosphere due to increased evaporation from the ocean as a result of a warmer climate and thus an increase in the latent heat flux to the atmosphere. The moister atmosphere hypothesis (Lambert, 1994, 1996, Lim & Simmonds, 2002, 2004, Sinclair, 1999, Hall, 1994, Zhang & Wang, 1997, Carnell, 1996) likely plays a major role in affecting surface and upper level cyclogenesis, storm maintenance, and cyclolysis (Carnell, 1996, 1998, Hall, 1994, Knipperitz et al., 2000, Lim & Simmonds, 2002, 2004, Lambert, 1995, 1996). Without the increased moisture in the atmosphere in a warmer climate, there probably would be a drastic decrease of ICEs due to the greatly reduced low level hemispheric baroclinicity.

Diabatic heating changes in a warmer climate, specifically the latent heat flux from the surface into the atmosphere would create a dramatically moister low-level atmosphere that could potentially lead to some of the largest changes. This often forgotten but extremely influential term, the latent heat flux, quite possibly could have as large if not a larger effect upon changes in NH extratropical cyclone intensity, duration, and geographical distribution as baroclinicity itself in a doubled CO₂ environment (Lambert, 1996, 1998, Lim & Simmonds, 2002, 2004, Geng & Sugi, 2002, 2003, Knipperitz et al., 2000). Large amounts of excess water vapor in the atmosphere can be viewed upon as the extra coal to a cyclone's engine to keep them forming and intensifying despite a hemispheric decrease in baroclinicity. The energetic mechanism by which ICEs develop may be the most significant change

in the doubled CO₂ environment. Since that environment is characterized by a reduction in meridional baroclinicity and yet the same number of ICEs occur, it seems likely that diabatic effects associated with the phase change of water must play an even greater role in cyclone development in the doubled CO₂ environment than in the present environment. Such a significant change in the developmental mechanism might be directly tied to a major change in cyclone structure. Pursuit of this intriguing question is left to future work. In future studies to enhance the results shown here, different and/or finer resolution models could be used accompanied with longer datasets with more model-outputted variables. The verdict is still out on how "exactly" increased greenhouse gases in the atmosphere will effect NH extratropical storms. Despite this, this presentation hopes to show that to study intense cyclone events, looking at merely the total number of events apparently does not nearly tell the story.

6. References

- Carnell, R. E., C. A. Senior, J. F. B. Mitchell, 1996. An assessment of measures of storminess: simulated changes in northern hemisphere winter due to increasing CO₂. *Clim. Dyn.*, **12**, 467-476.
- _____, and _____, 1998. Changes in mid-latitude variability due to increasing greenhouse gases and sulphate aerosols. *Clim. Dyn.*, **14**, 369-383.
- Chang, E. K. M., I. Orlanski, 1993. On the Dynamics of a Storm Track. *J. Atmos. Sci.*, **50**, 999-1015.
- _____, S. Lee, K. L. Swanson, 2002. Storm Track Dynamics. *J. Climate*, **15**, 2163-2183.
- _____, and Y. Fu, 2002. Interdecadal Variations in Northern Hemisphere Winter Storm Track Intensity. *J. Climate*, **15**, 642-658.
- Delworth, T. L., et al., submitted 2004. GFDL's CM2 global coupled climate models – Part 1: formulation and simulation characteristics. Submitted to *J. Climate*.
- Geng, Q. and M. Sugi, 2001. Variability of the North Atlantic cyclone activity in winter analyzed from NCEP-NCAR Reanalysis data. *J. Climate*, **14**, 3863-3873.
- _____, and _____, 2003. Possible change of extratropical cyclone activity due to enhanced greenhouse gases and sulfate aerosols – Study with a high-resolution AGCM. *J. Climate*, **16**, 2262-2274.
- Hall, N. M. J., B. J. Hoskins, P. J. Valdes, and C. A. Senior, 1994. Storm tracks in a high resolution GCM

- with doubled carbon dioxide. *Q. J. R. Meteorol. Soc.*, **120**, 1209-1230.
- Hartmann, D. L., 1994. *Global physical climatology*, Academic Press (San Diego).
- Holton, J. R., 1992. *An introduction to dynamic meteorology*, Academic Press (San Diego).
- IPCC, 2001. *Climate Change 2001, the scientific basis*, WMO/UNEP.
- Knipperitz, P., U. Ulbrich, and P. Speth, 2000. Changing cyclones and surface wind speeds over the North Atlantic and Europe in a transient GHG experiment. *Clim. Res.*, **15**, 109-122.
- König, W., R. Sausen, F. Sielmann, 1993. Objective identification of cyclones in GCM simulations. *J. Climate*, **6**, 2217-2231.
- Lambert, S. J. 1995: The effect of enhanced greenhouse warming on winter cyclone frequencies and strengths. *J. Climate*, **8**, 1447-1452.
- _____, 1996. Intense extratropical northern hemisphere winter cyclone events: 1899-1991. *J. Geophys. Res.*, **101**, 21,319-21,325.
- Lau, N.-C., 1988. Variability of the observed midlatitude storm tracks in relation to low-frequency changes in the circulation pattern. *J. Atmos. Sci.*, **45**, 2718-2743.
- Lim, E.-P., and I. Simmonds, 2002. Explosive cyclone development in the southern hemisphere and a comparison with northern hemisphere events. *Mon. Wea. Rev.*, **130**, 2188-2209.
- _____, and _____, 2003. Changes to the vertical structure of cyclones under global warming. *7th International Conference on the SH Meteorology and Oceanography*, Wellington, New Zealand, 24-28 March 2003.
- _____, and _____, 2004. Assessment of changes in winter extratropical cyclones with increasing CO₂. *The 84th American Meteorological Society annual meeting*, Seattle, WA 10-15 January 2004.
- Lunkeit, F., K. Fraedrich, and S. E. Bauer, 1998. Storm tracks in a warmer climate: sensitivity studies with a simplified global circulation model. *Clim. Dyn.*, **14**, 813-826.
- Magnusdottir, G., C. Deser, and R. Saravanan, 2004. The effects of North Atlantic SST and sea ice anomalies on the winter circulation in CCM3, Part I: Main features and storm track characteristics of the response. *J. Climate*, **17**, 857-876.
- Martin, J. E., 2005. Personal Communication.
- Peixoto, J. P. and A. H. Oort, 1992. *Physics of climate*, American Institute of Physics (New York).
- Sutcliffe, R. C., 1947. A contribution to the problem of development. *Quart. J. Roy. Meteor. Soc.*, **73**, 370-383.
- Shubert, M., J. Perlwitz, R. Blender, K. Fraedrich, and F. Lunkeit, 1998. North Atlantic cyclones in CO₂-induced warm climate simulations: frequency, intensity, and tracks. *Clim. Dyn.*, **14**, 827-837.
- Sinclair, M. R. and I. G. Watterson, 1999. Objective assessment of extratropical weather systems in simulated climates. *J. Climate*, **12**, 3467-3485.
- The GFDL Global Atmospheric Model Development Team, 2004. The new GFDL global atmosphere and land model AM2-LM2: evaluation with prescribed SST simulations. *J. Climate*, **17**, 4641-4673.
- Uccellini, L. W., 1990. Processes contributing to the rapid development of extratropical cyclones. *Extratropical Cyclones: The Erik Palmén Memorial Volume*, C. W. Newton and E. O. Holopainen, Eds., Amer. Meteor. Soc., 81-105.
- Vavrus, S. J., 2005. Personal Communication.
- Weaver, C. P., 1999. The interactions among cyclone dynamics, vertical thermodynamic, structure, and cloud radiative forcing in the North Atlantic summertime storm track. *J. Climate*, **12**, 2625-2642.
- Zhang, X., J. E. Walsh, J. Zhang, U. S. Bhatt, and M. Ikeda, 2004. Climatology and interannual variability of artic cyclone activity: 1948-2002. *J. Climate*, **17**, 2300-2317.
- Zhang, Y. and W.-C. Wang, 1997. Model simulated northern winter cyclone and anticyclone activity under a greenhouse warming scenario. *J. Climate*, **10**, 1616-1634.